

# Two-Dimensional Modeling of Guided Ultrasound Wave Propagation in Intact and Healing Bones Immersed in Fluid

Maria G. Vavva, Vasilios C. Protopappas, *Member, IEEE*, Dimitrios I. Fotiadis, *Member, IEEE*, and Demos Polyzos

**Abstract**—Guided wave propagation has gained significant interest in the ultrasonic evaluation of bone. Previous computational and experimental studies are based on the theory describing guided wave propagation in a free two-dimensional plate (Lamb wave theory). In this work, we modify the boundary conditions so as to take the effect of the overlying soft tissues into account. A two-dimensional model of a bone-mimicking plate (density  $1500\text{Kg/m}^3$ , Young's modulus  $14\text{GPa}$ , cortical thickness  $4\text{mm}$ ) was developed. The fracture callus tissue was modeled as an inhomogeneous material consisting of six ossification regions with properties changing during the healing period. The bone was assumed immersed in blood (fluid-loaded boundary conditions). The ultrasound transmitter and receiver ( $1\text{MHz}$ ) were placed on each side of the callus, equidistant from it at a  $35\text{mm}$  in-between distance. First, we investigated the propagation velocity of the first arriving signal (FAS) using traditional time-domain analysis. Next, the velocity dispersion of the guided wave modes was represented in the time-frequency (t-f) domain of the signal. Characterization of the propagating guided modes was carried out by incorporating the theoretical leaky Lamb wave dispersion curves. Comparing with previous results obtained from free intact and healing plates, it was found that the surrounding soft tissues have a significant effect on the dispersion of guided waves. The effect was less pronounced on the FAS propagation velocity. However, leaky Lamb waves were again sensitive to the material and mechanical changes during the simulated healing process. In conclusion, the application of realistic boundary conditions provides an improved approach to interpreting clinical measurements.

## I. INTRODUCTION

Quantitative determination of bone mechanical properties is a crucial issue not only for the assessment of degenerative diseases such as osteoporosis, but also for

Manuscript received June, 30, 2006.

M. G. Vavva is with the Department of Material Science and Engineering, University of Ioannina, and the Unit of Medical Technology and Intelligent Information Systems, Computer Science Department, University of Ioannina, GR 45 110 Ioannina, Greece (e-mail: mvavva@cc.uoi.gr).

V. C. Protopappas is with the Department of Medical Physics, Medical School, University of Ioannina and the Unit of Medical Technology and Intelligent Information Systems, Computer Science Department, University of Ioannina, GR 45 110 Ioannina, Greece (e-mail: me00642@cc.uoi.gr).

D. I. Fotiadis is with the Unit of Medical Technology and Intelligent Information Systems, Computer Science Department, University of Ioannina, Greece, and also with the Biomedical Research Institute – FORTH, GR 45 110 Ioannina, Greece (e-mail: fotiadis@cs.uoi.gr).

D. Polyzos is with the Department of Mechanical Engineering and Aeronautics, University of Patras, GR 26 500, Greece (e-mail: polyzos@mech.upatras.gr).

the objective evaluation of fracture healing. The so-called axial transmission technique has been developed to serve that purpose by measuring the ultrasound velocity of the waves propagating through the long axis of the bone. This technique allows for the evaluation of long bones like tibia and radius. A transmitter and a receiver are placed along the bone axis either in contact with the skin [1] or through implantation directly onto the bone surface [2,3]. The apparent velocity is specified by the transit time of the first arriving signal (FAS) at the receiver and the propagation distance.

The correlation between the FAS velocity and the properties of bone, such as mineral density, cortical thickness and elastic modulus, has been clarified experimentally [4,5] and by computed simulations [6-9]. Clinical [10] and animal [2,3] research, as well as simulations of two-dimensional (2-D) bone models [11], aiming at the assessment of the fracture healing process, have indicated that the FAS velocity increases during the healing period. In addition, both experimental immersion techniques on acrylic plates and *in vivo* applications [12] have been carried out in order to elucidate the effect of the surrounding soft tissue and the width of the fracture gap on the FAS propagation velocity.

However, the FAS wave corresponds to a “surface wave” when the wavelength is smaller than the thickness of the cortex, and therefore its velocity reflects only the properties of the cortex along a subsurface region. Conversely, when the wavelength of the transmitted wave is larger than the cortical thickness, the bone acts as a waveguide supporting the propagation of guided wave modes [13]. Guided waves have recently been regarded as a significant tool in the ultrasound evaluation of bone status since they are sensitive to both the mechanical and geometrical properties of the propagation medium. Computational studies on 2-D bone models [6,9] and experimental research [4,9,14,15] have been performed to investigate guided wave propagation by making use of the Lamb wave theory (the theory that describes guided waves in free 2-D plates) [13]. As opposed to the above mentioned studies which focused on osteoporosis, we recently demonstrated that guided waves can be also useful in monitoring the fracture healing process [1]. A free 2-D isotropic healing bone model was developed and the investigation of guided wave propagation was based on time-frequency (t-f) signal analysis. However, all the above-mentioned studies have neglected the effect of the

surrounding soft tissues on guided wave propagation. The soft tissues provide a leakage path for the ultrasonic energy giving rise to the so-called leaky wave modes.

In this work, we extend our previous 2D computational study by taking into account more realistic conditions. The presence of the soft tissues is simulated by immersing the bone-mimicking plate in fluid. Also, the model of the healing bone is enhanced by considering the callus tissue as an inhomogeneous material consisting of six different ossification regions. Our main objective is to investigate the influence of the overlying soft tissue on the characteristics of guided wave propagation. In this respect, we perform two series of simulations. In the first (SeriesI), the bone is considered free, whereas in the second (SeriesII) the bone is assumed to be immersed in blood. We first investigate the difference in the FAS velocity between the two series of simulations. Then, we analyze the signals in the t-f domain to obtain represent the dispersion of the guided waves. Detection of the modes in the t-f domain is performed by superimposing theoretical dispersion curves computed (a) for the Lamb modes (SeriesI) and (b) for the leaky Lamb modes (SeriesII). By comparing the data obtained from the two series, we demonstrate that the surrounding soft tissues affect the dispersion of guided waves and are thus a significant parameter that must be included in the bone models.

To our knowledge no previous work has reported on the use of leaky guided waves in the study of bone fracture healing.

## II. GUIDED WAVES IN A PLATE

Wave propagation through bounded media results in multiple reflections of the waves at the boundaries and mode conversion occurs between longitudinal (compression) and shear (transverse) waves. As the waves propagate in the medium, superpositions cause the formation of wave packets which are called guided wave modes. Guided waves are dispersive, i.e. the velocity at which a wave mode propagates within a medium is a function of the frequency.

In the case of a homogeneous isotropic elastic plate with traction-free upper and lower surfaces (the free plate problem), the guided waves are called plate modes or Lamb modes [13]. The Lamb modes are divided into symmetric modes (denoted as  $S_n$ , where  $n=0,1,\dots$ ) and anti-symmetric modes (denoted as  $A_n$ ,  $n=0,1,\dots$ ). The dispersion of Lamb modes is described by a transcendental equation known as the Rayleigh-Lamb frequency equation. The roots of the characteristic equation relate the group velocity of a mode to the frequency and are provided in the form of group velocity dispersion curves.

When the plate is immersed in a fluid, the boundary conditions of the problem are modified to accommodate the fluid-loading conditions at the upper and lower surfaces of the plate. In this case, the modes are called leaky Lamb modes (denoted respectively as  $l-S_n$  and  $l-A_n$ ,  $n=0,1,\dots$ ) and

their dispersion curves are derived from the (modified) frequency equation. Fig. 1 depicts the group velocity dispersion curves for a bone-mimicking plate in two cases: (a) free or (b) immersed in fluid (blood).

## III. MATERIALS AND METHODS

### A. Bone Model

The cortical bone was assumed to be a linear elastic isotropic plate with Young's modulus  $E_{bone}=14$  GPa, as measured in a previous experimental animal study [2]. The Poisson' ratio was  $\nu_{bone}=0.37$ , which is a typical value for bone [6,7,9,11]. The bone was considered a homogeneous material with  $\rho_{bone}=1500$  Kg/m<sup>3</sup> [2]. The cortical thickness was 4 mm (which is close to some types of human long bones [6,9,11]). The bulk longitudinal,  $c_L$ , and shear,  $c_T$ ,

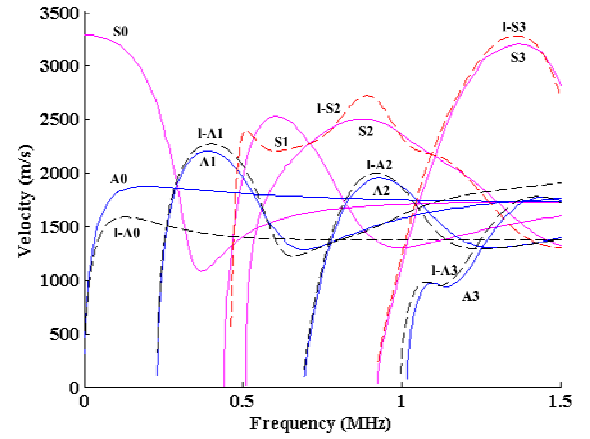


Fig. 1. Group velocity dispersion curves of the Lamb modes for a free plate (solid lines) and for a plate immersed in blood (dashed lines). The bulk longitudinal and shear velocity of the plate was 4063 m/s and 1846 m/s, respectively, and the plate thickness was 4 mm.

velocities of the bone were calculated as [13]:

$$c_L = \sqrt{\frac{E(1-\nu)}{\rho(1+\nu)(1-2\nu)}}, \quad (1)$$

$$c_T = \sqrt{\frac{E}{2\rho(1+\nu)}}, \quad (2)$$

and were found 4063 m/s and 1846 m/s, respectively.

### Model of Fracture Callus

Based on a previous computational study [16], we modeled the fracture callus tissue as an inhomogeneous material consisting of six distinct ossification regions, denoted as I, II, ..., VI (Fig. 2). The geometry of the callus was described by an endosteal and a periosteal region which are designed outside and inside the borders of the plate. To represent the process of the progressive differentiation and stiffening of the callus tissue, which occurs in the secondary type of fracture healing, we assumed the following tissue

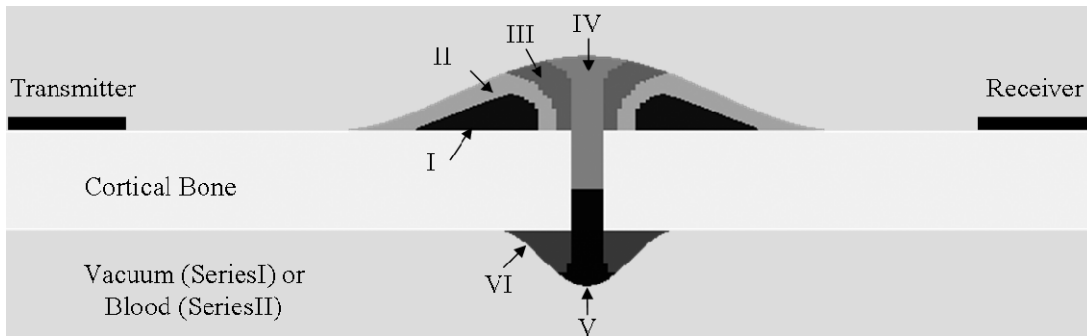


Fig. 2. The model of the healing bone along with the transmitter-receiver configuration. The capital Latin numbers correspond to the six different ossification regions that comprise the callus tissue. The bone is in vacuum (SeriesI) or surrounded by blood (SeriesII).

types to be involved in the process: initial connective tissue (ICT), soft callus (SOC), intermediate stiffness callus (MSC), stiff callus (SC) and ossified tissue (OT). We assumed that healing progresses in three stages. At Stage1, the callus contained regions of MSC along the endosteal and periosteal surfaces of cortex at some distance from the fracture gap (i.e. in regions I and VI), SOC adjacent to them (regions II and V), while the remainder was occupied by ICT (regions III and IV). At Stage2, the callus consisted of ICT (in region IV), SOC (in region III), MSC (in region II) and SC (in regions I, V and VI). Finally at Stage3, bone formation has been almost completed and thus the callus tissue consisted of OT except for two regions filled with SC (region III) and SOC (region IV). A hypothetical “zero” stage (Stage0) was used to examine the influence of the callus geometry itself on the characteristics of wave propagation. In this stage, all the callus regions were assumed to be composed of cortical bone. All the soft tissue types were assumed isotropic and their material properties

TABLE I  
MATERIAL PROPERTIES OF THE TYPES OF SOFT TISSUES INVOLVED IN THE HEALING PROCESS

Tissue Type	Density (Kg/m <sup>3</sup> )	Young's Modulus (MPa)	Poisson's ratio	Bulk Longitudinal Velocity (m/s)
ICT	1050	3	0.4998	1543
SOC	1100	1000	0.47	2337
MSC	1200	3000	0.45	3079
SC	1250	6000	0.43	3697
OT	1400	10000	0.40	3912

are presented in Table I.

#### A. Axial-Transmission

A transmitter and a receiver were placed in contact with the plate's upper surface, equidistant from the fracture callus. The contact area of the transducers was 5mm and their center-to-center distance was 35 mm, which is a typical value used in ultrasonic studies of bone [2,6,9,11]. The excitation signal was described by a 3-cycle Gaussian-modulated 1MHz sine. The transducers operated in the longitudinal mode.

#### B. Boundary Conditions

Two Series of simulations were performed. In SeriesI, the bone model was in vacuum (free boundary conditions). In SeriesII, the bone model was immersed in blood in order to take into account the effect of the surrounding soft tissues. In both series, absorbing boundary conditions were applied at the left and right sides of the plate in order to eliminate the interference from the reflections which correspond to an infinitely-long plate.

#### C. Simulation Method

Numerical solution to the 2-D wave propagation problem was performed with the finite difference method using the commercial software Wave2000 Pro (CyberLogic, Inc., NY, USA). The element size was set at 0.1 mm which corresponds to at least ten elements per smallest wavelength. The sampling frequency was 46.97 MHz. The duration of the recorded signals was 110  $\mu$ s.

#### D. Time-Domain Analysis

The ultrasound propagation velocity was determined by dividing the transducers' in-between distance to the transition time of the FAS. The FAS was detected in the signal waveform by using a threshold equal to 10% of the amplitude of the first signal extremum [2, 6, 9, 11].

#### E. Time-Frequency Domain Analysis

T-f signal analysis has been previously used for representing the velocity dispersion of the Lamb modes in non-destructive testing applications [17,18]. Contrary to traditional time domain and 2-D Fourier transform techniques, t-f analysis requires only a broadband excitation to represent the dispersion of multiple wave modes.

In the present work, we used the reassigned Smooth-Pseudo Wigner-Ville (RSPWV) energy distribution function since it has been previously found effective in representing and localizing guided waves [11].

## IV. RESULTS

The propagation velocity of the FAS wave was found 3914 m/s for the intact bone model in both SeriesI and

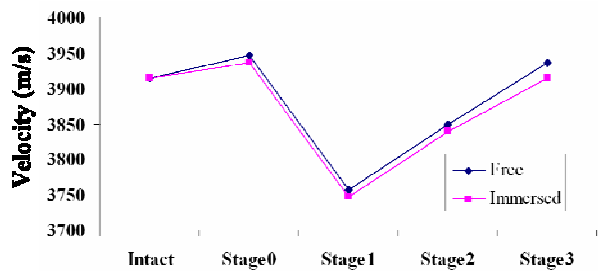


Fig. 3. Evolution of the FAS propagation velocity throughout the healing progress of the model in SeriesI and SeriesII.

SeriesII. Since the velocity was close to the bulk velocity of the bone (4063 m/s), the FAS corresponds to a lateral wave rather to a guided wave. The evolution of the FAS velocity over the simulated healing stages in SeriesI and II is illustrated in Fig. 3.

Snapshots of wave propagation in the healing bone at Stage2 in SeriesII recorded at 3  $\mu$ s, 10  $\mu$ s, and 17  $\mu$ s are presented in Fig. 4. It can be seen that in addition to the waves propagating in the bone, waves are also radiated into

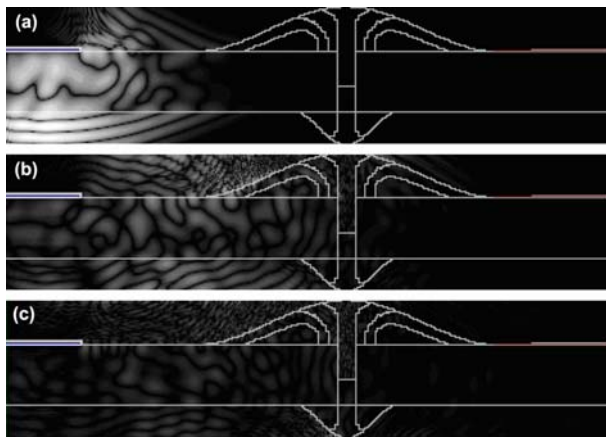


Fig. 4. Three snapshots of wave propagation in the healing bone at Stage2 in SeriesII recorded at (a) 3  $\mu$ s, (b) 10  $\mu$ s, and (c) 17  $\mu$ s.

the fluid. When the waves arrive at the callus, the wavelengths in each region become different depending on the properties of the soft tissues. Complicated phenomena and multiple reflections occur at the boundaries of the callus regions. Due to the energy leakage into the fluid, the received waves are highly attenuated compared to those in SeriesI.

The t-f signal representations of the signals obtained from the intact bone model in SeriesI and II are illustrated in Figs. 5(a) and (b), respectively. The t-f representations are shown in the form of pseudo-color 2-D images, where the color of a point represents the amplitude (in dB) of the energy distribution. In order to identify the propagating guided modes in the t-f representation, we superimposed on each image the corresponding theoretical velocity dispersion curves. From Fig. 5(a), it can be observed that in the free intact bone two Lamb modes were dominant, namely the S2 mode with dispersion identified in the 0.55 - 0.8 MHz frequency range and the A3 with dispersion from its cut-off

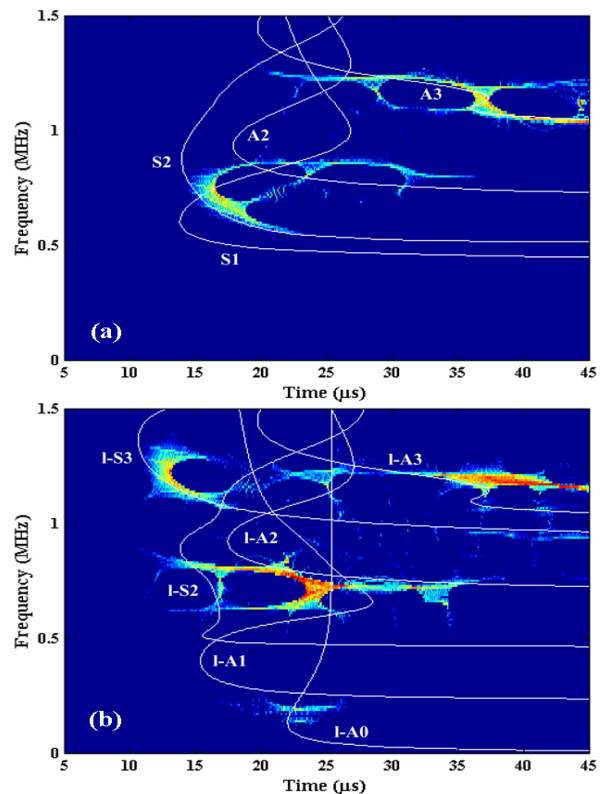


Fig. 5. T-f representations of the signals obtained from the intact model (a) in SeriesI and (b) in SeriesII. The corresponding theoretical dispersion curves are also superimposed on each image.

frequency (1.05 MHz) up to 1.25 MHz. The situation was different in the immersed intact bone (Fig. 5(b)). The dispersion curves clearly characterized the I-S3 and I-A3 modes, whereas the propagation of some other modes, such as the I-A0 and I-S2, was poorly supported.

The t-f representations of the signals obtained from the simulated healing stages in SeriesI and SeriesII are illustrated in Fig. 6 and Fig.7, respectively. It can be seen that the geometrical disturbance induced by the callus at Stage0 affected the dispersion of the S2 and A3 modes in

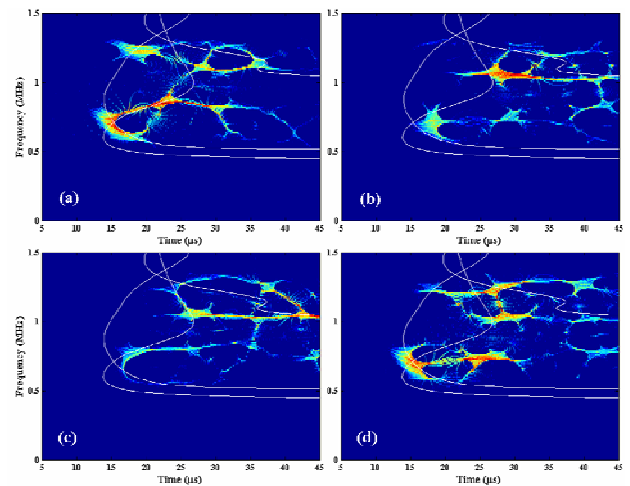


Fig. 6. T-f representations of the signals obtained from the healing bone in SeriesI at (a) Stage0, (b) Stage1, (c) Stage2, and (d) Stage3.

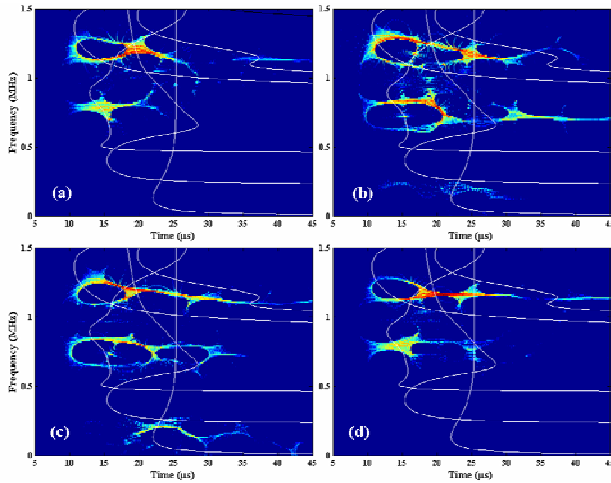


Fig. 7. T-f representations of the signals obtained from the healing bone in SeriesII at (a) Stage0, (b) Stage1, (c) Stage2, and (d) Stage3.

SeriesI (Fig. 6(a)) and of the I-S3 and I-A3 in SeriesII (Fig. 7(a)). In both cases, additional waves appeared which did not correspond to any theoretical mode and can be possibly attributed to reflections caused by the callus geometry. The dispersion of the modes was also sensitive to the material changes that took place from Stage1 to Stage3.

## V. DISCUSSION

We presented a numerical study on guided ultrasound wave propagation in intact and healing long bones. The effect of the surrounding soft tissues on the propagation velocity of the FAS wave and on the dispersion of guided waves was evaluated by comparing two different boundary conditions.

We developed a 2D bone model similar to that developed in our previous work [11] and to those reported in osteoporosis studies [6,9]. We extended the model of callus by incorporating several ossification regions. Three stages were used to simulate progress of bone healing. According to [16], Stage1 and Stage2 correspond to the fourth and eighth week after fracture, respectively, whereas Stage3 reflects the phase before bone remodeling. Although those stages represent critical phases of the healing course, the early stage of haematoma development and the gradual reduction in the dimensions of callus as a result of the bone remodeling process were not taken into account.

Although the presented model is enhanced in terms of realistic boundary conditions, compared to previous studies, many simplified assumptions were adopted. These include that bone and callus were assumed elastic materials, and their anisotropic properties were not taken into account.

For 1-MHz excitation the wavelength in the bone (approximately 4mm) was comparable to the cortical thickness. We showed that the FAS wave propagated in the intact bone models (both free and blood-loaded) as a non-dispersive lateral wave, since its velocity was found to be close to the nominal bulk velocity of bone. Also, the blood-loading conditions did not affect the velocity of the FAS in

the intact model. When the callus was incorporated in the bone model, the FAS velocity increased during the simulated healing process, which is in agreement with our previous study [11]. The velocity at each healing stage was found slightly lower in SeriesII, however its evolution over the stages remained the same. The FAS wave corresponds to a lateral wave which according to [5,7] propagates only along 1.4 mm deep layer at 1 MHz. As such, its velocity of propagation does not reflect the properties of the endosteal and periosteal callus regions.

However, the broadband excitation that was utilized supported the generation of multiple guided modes that depend on the properties of the whole medium. We analyzed our signals by means of t-f signal analysis techniques. The simulated dispersion of guided modes in the intact bone was found to be modified when fluid boundary conditions were taken into consideration. More specifically, in the free intact bone the S2 and A3 modes propagated, whereas in the immersed bone the dominant modes were the I-A3, I-S3. Therefore, the propagation of guided waves is greatly affected by the boundary conditions of the problem.

For the healing bone, we found that the propagating free and leaky guided waves were influenced by both geometrical and mechanical properties of the callus. The significant effect of callus geometry on mode propagation was assessed separately at Stage0 in both series of simulations. We also showed that mode dispersion was influenced by the material properties of callus at each stage. However, at Stage3 the dispersion of the modes gradually returned to that observed at Stage0. Since guided waves can reflect geometrical and structural changes that take place throughout the cortical thickness, they can offer an improved means of monitoring bone fracture healing.

## VI. CONCLUSIONS

We performed a numerical study of wave propagation in a healing bone which was simulated as a 2-D infinite plate immersed in blood. It was well understood from the model that the surrounding soft tissues have great impact on guided wave propagation, both in the intact and in the healing bone. This is justified by the fact that they provide leakage paths for the ultrasonic waves resulting in modified dispersion curves compared to those derived from a free plate. Therefore, the application of realistic boundary conditions is crucial to interpret clinical measurements. Nevertheless, further research is needed in order to investigate the effect of anisotropy and irregular geometry of bone on the characteristics of wave propagation. Three-dimensional bone models taking into consideration such realistic parameters need to be developed.

## REFERENCES

- [1] E. Bossy, M. Talmant, M. Defontaine, F. Patat, and P. Laugier, "Bidirectional axial transmission can improve accuracy and precision of ultrasonic velocity measurement in cortical bone: A validation on

- test materials," *IEEE Trans. Ultrason. Ferroelectr. Freq. Control*, vol. 51, no. 1, pp. 71-79, 2004.
- [2] V. C. Protopappas, D. Baga, D. I. Fotiadis, A. Likas, A. A. Papachristos, and K. N. Malizos, "An ultrasound wearable system for the monitoring and acceleration of fracture healing in long bones," *IEEE Trans. Biomed. Eng.*, vol. 52, no. 9, pp. 1597-1608, 2005.
- [3] K. N. Malizos, A. A. Papachristos, V. C. Protopappas, and D. I. Fotiadis, "Transosseous Application of Low-Intensity Ultrasound for the Enhancement and Monitoring of Fracture Healing Process in a Sheep Osteotomy Model," *Bone*, vol. 38, no. 4, pp. 530-539, 2006.
- [4] P. Moilanen, P. H. F. Nicholson, T. Kärkkäinen, Q. Wang, J. Timonen, and S. Cheng, "Assessment of the tibia using ultrasonic guided waves in pubertal girls," *Osteoporosis Int.*, vol. 14, pp. 1020-1027, 2003.
- [5] K. Raum, I. Leguerney, F. Chandelier, E. Bossy, M. Talmant, A. Saïed, F. Peyrin, and P. Laugier, "Bone microstructure and elastic tissue properties are reflected in QUS axial transmission measurements," *Ultrasound Med. Biol.*, vol. 31, no. 9, pp. 1225-1235, 2005.
- [6] E. Bossy, M. Talmant and P. Laugier, "Effect of cortical thickness on velocity measurements using ultrasonic axial transmission: a 2D simulation study," *J. Acoust. Soc. Am.*, vol. 112, no. 1, pp. 297-307, July, 2002.
- [7] E. Bossy, M. Talmant, and P. Laugier, "Three-dimensional simulations of ultrasonic axial transmission velocity measurement on cortical bone models," *J. Acoust. Soc. Am.*, vol. 115, no. 5, pp. 2314-2324, 2004.
- [8] E. Camus, M. Talmant, G. Berger and P. Laugier, "Analysis of the axial transmission technique for the assessment of skeletal status," *J. Acoust. Soc. Am.*, vol. 108, no. 6, pp. 3058-3065, December, 2000.
- [9] P. H. F. Nicholson, P. Moilanen, T. Kärkkäinen, J. Timonen and S. Cheng, "Guided ultrasonic waves in long bones: modeling, experiment and in vivo application", *Phys. Meas.*, vol. 23, pp. 755-768, 2002.
- [10] J. L. Cunningham, J. Kenwright and C. J. Kershaw, "Biomechanical measurement of fracture healing," *J. Med. Eng. Tech.*, vol. 13, no. 3, pp. 92-101, 1990.
- [11] V. C. Protopappas, D. I. Fotiadis, and K. N. Malizos, "Guided ultrasound wave propagation in intact and healing long bones," *Ultrasound Med. Biol.*, vol. 32, no. 5, pp. 693-708, 2006.
- [12] G. Lowet and G. Van Der Perre, "Ultrasound velocity measurements in long bones: measurement method and simulation of ultrasound wave propagation," *J. Biomech.*, vol. 29, no. 10, pp. 1255-1262, 1996.
- [13] J. L. Rose, *Ultrasonic waves in solid media*. Cambridge: Cambridge University Press, 1999.
- [14] F. Lefebvre, Y. Deblock, P. Campistron, D. Ahite, and J. J. Fabre, "Development of a new ultrasonic technique for bone and biomaterials in vitro characterization," *J. Biomed. Mater. Res.*, vol. 63, no. 4, pp. 441-446, 2002.
- [15] K. I. Lee, and S. W. Yoon, "Feasibility of bone assessment with leaky Lamb waves in bone phantoms and a bovine tibia," *J. Acoust. Soc. Am.*, vol. 115, no. 6, pp. 3210-3217, 2004.
- [16] L. E. Claes, and C. A. Heigele, "Magnitudes of local stress and strain along bony surfaces predict the course and type of fracture healing," *J. Biomech.*, vol. 32, no. 3, pp. 255-266, 1999.
- [17] M. Niethammer, L. J. Jacobs, J. Qu, and J. Jarzynski, "Time-frequency representations of Lamb waves," *J. Acoust. Soc. Am.*, vol. 109, no. 5, pp. 1841-1847, 2001.
- [18] W. H. Proseer, M. D. Seale, and B. T. Smith, "Time-frequency analysis of the dispersion of lamb modes," *J. Acoust. Soc. Am.*, vol. 105, no. 5, pp. 2669-2676, 1999.